



**HAL**  
open science

# Identification and characterization of the main peptides in pea protein isolates using ultra high-performance liquid chromatography coupled with mass spectrometry and bioinformatics tools

Audrey Cosson, Lydie Oliveira Correia, Nicolas Descamps, Anne Saint-Eve,  
Isabelle Souchon

## ► To cite this version:

Audrey Cosson, Lydie Oliveira Correia, Nicolas Descamps, Anne Saint-Eve, Isabelle Souchon. Identification and characterization of the main peptides in pea protein isolates using ultra high-performance liquid chromatography coupled with mass spectrometry and bioinformatics tools. *Food Chemistry*, 2022, 367, pp.130747. 10.1016/j.foodchem.2021.130747 . hal-03517046

**HAL Id: hal-03517046**

**<https://hal.inrae.fr/hal-03517046v1>**

Submitted on 2 Aug 2023

**HAL** is a multi-disciplinary open access archive for the deposit and dissemination of scientific research documents, whether they are published or not. The documents may come from teaching and research institutions in France or abroad, or from public or private research centers.

L'archive ouverte pluridisciplinaire **HAL**, est destinée au dépôt et à la diffusion de documents scientifiques de niveau recherche, publiés ou non, émanant des établissements d'enseignement et de recherche français ou étrangers, des laboratoires publics ou privés.

1 **Title:** Identification and characterization of the main peptides in pea protein isolates using ultra high-  
2 performance liquid chromatography coupled with mass spectrometry and bioinformatics tools

3 **Authors:** Audrey Cosson<sup>ab</sup>, Lydie Oliveira Correia<sup>c</sup>, Nicolas Descamps<sup>b</sup>, Anne Saint-Eve<sup>a</sup>, Isabelle  
4 Souchon<sup>d\*</sup>

5 **Affiliations**

6 <sup>a</sup>Univ Paris Saclay, UMR SayFood, AgroParisTech, INRAE, F-78850 Thiverval Grignon, France.

7 <sup>b</sup>Roquette Frères, 10 rue haute loge, F-62136, Lestrem, France

8 <sup>c</sup>Univ Paris Saclay, INRAE, AgroParisTech, Micalis Inst,PAPPSO, F-78350 Jouy En Josas, France

9 <sup>d</sup>Avignon Univ, UMR SQPOV, INRAE, F-84000 Avignon, France

10 **\*Corresponding author:** Isabelle Souchon, Phone: +33 (0)4 32 72 24 89, Address: UMR408 SQPOV  
11 - Sécurité et Qualité des Produits d'Origine Végétale, Domaine Saint Paul, 228, route de  
12 l'Aérodrome, Site Agroparc - CS 40509, 84914 Avignon Cedex 9, FRANCE

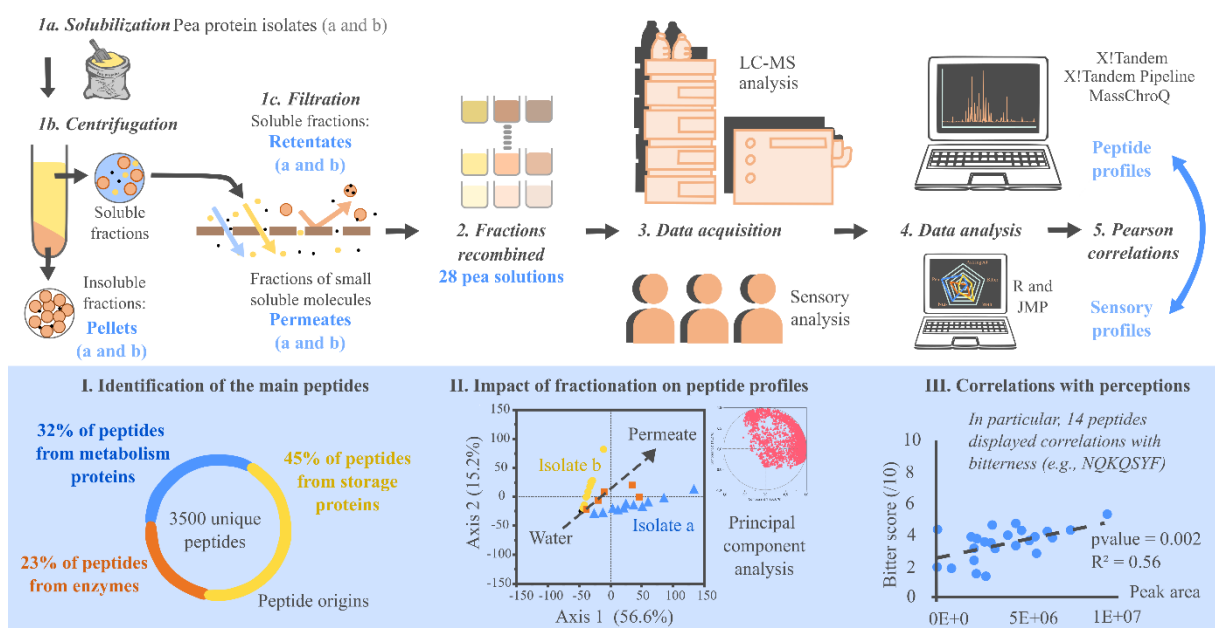
13 **Email:** [isabelle.souchon@inrae.fr](mailto:isabelle.souchon@inrae.fr)

14 **Email addresses for co-authors:**

15 [audrey.cosson@inrae.fr](mailto:audrey.cosson@inrae.fr) ; [lydie.oliveira-correia@inrae.fr](mailto:lydie.oliveira-correia@inrae.fr) ; [nicolas.descamps@roquette.com](mailto:nicolas.descamps@roquette.com) ;

16 [anne.saint-eve@inrae.fr](mailto:anne.saint-eve@inrae.fr)

17 **Graphical abstract:**



18

19 **Highlights**

- 20 • 3,005 unique peptides identified in pea protein solutions
- 21 • 45% of peptides came from seed storage proteins, mainly vicilins
- 22 • 11 peptides displayed sequence homology with known antioxidants
- 23 • 1,640 peptides were associated with high broth scores, perhaps reflecting umami
- 24 • 14 peptides appeared to influence the perception of bitterness

25

26 **Abstract:**

27 Pea protein isolates are a source of high-quality plant proteins. However, from a sensory perspective,  
28 they are usually described as having strong beany and bitter notes, which arise from a complex  
29 mixture of volatiles, phytochemicals, and peptides. The aim of this study was to identify the main  
30 peptides in isolates and examine their correlations with sensory perceptions. Thus, 28 solutions  
31 containing different mixtures of pea protein fractions were assessed. Any peptides present were  
32 identified and characterized using ultra high-performance liquid chromatography-mass spectrometry.  
33 There were a total of 3,005 unique peptides representing various protein families; 1,640 and 275  
34 peptides were correlated with broth and bitter attributes, respectively. In particular, 14 peptides with  
35 short sequences (< 8 residues) were correlated with bitterness. These results show how key peptides in  
36 isolates may cause sensory perceptions.

37 **Keywords:** pulse, peptidomics, bitter, beany, sensory, correlations

38

39 **1. Introduction**

40 A major recent challenge in the agrifood industry is developing new protein sources to compensate for  
41 the anticipated future paucity of traditional animal proteins. Consequently, both the industry and  
42 consumers are focusing their attention on plant proteins. Plant protein isolates, such as those derived  
43 from peas (*Pisum sativum* L.), are often used to create foods because of their functional properties,  
44 protein content, sustainable production, and relatively low cost (Davis et al., 2010). However, plant  
45 proteins, and especially isolate fractions from raw plant matter, have some drawbacks from a sensory

46 point of view (e.g., their color, smell, and taste). It is necessary to better understand the sensory issues  
47 associated with plant proteins if we wish to develop plant protein-based foods that will be attractive to  
48 consumers.

49 Research on the perception of pea-based products has largely focused on the role of volatile aroma  
50 compounds in creating sensations of beaniness (Bi et al., 2020) and of phenolics/saponins in creating  
51 sensations of bitterness and astringency (Heng et al., 2006). However, it is important to carry out more  
52 detailed compositional analyses to clarify how foods are sensorily perceived.

53 Pea protein isolates are mainly composed of globulins, which are the main storage proteins in seeds.  
54 Globulins consist of two fractions that are characterized by their ultracentrifugation sedimentation  
55 coefficients: 7S (20%–40%) and 11S (20–30%). The 7S fraction is composed of vicilins and  
56 convicilins. The 11S fraction is composed of legumines (Creveu-Gabriel, 1999). During protein  
57 isolate extraction (notably during temperature and pH changes), proteins may be naturally hydrolysed  
58 into numerous peptides of different sizes (Li & Aluko, 2010; Sirtori et al., 2012). Several structural  
59 changes result because of the exposure of hydrophobic sites normally found in the protein's core  
60 (Daher et al., 2020). Although such peptides remain little studied, they could potentially have  
61 properties that might serve to improve the sensory properties of plant-based products.

62 Indeed, specific protein fragments may elicit various sensory perceptions (e.g., sweet, bitter, umami,  
63 sour, or salty notes). Sourness and saltiness could result from the presence of charged terminal groups  
64 and/or charged side chains (Temussi, 2012). Other perceptions (sweetness, umami, and bitterness)  
65 could be explained by the presence of different peptide families. For example, certain small peptides  
66 (5–8 residues in size) can activate the TAS2R bitter taste receptors in the mouth (Aubes-Dufau et al.,  
67 1995; Maehashi & Huang, 2009). These peptides tend to be hydrophobic with proline- and leucine-  
68 rich side chains, especially at their C-terminals (Kim et al., 2008). They can have quite an impact: for  
69 example, 0.25 mM of a peptide (VVYPWTQRF) solution derived from bovine hemoglobin elicits the  
70 same sensation of bitterness as 0.073 mM of quinine sulfate or 21 mM of caffeine (Aubes-Dufau et al.,  
71 1995). With regards to sweetness, there are no known natural peptides that result in sweet notes.

72 However, semi-synthetic peptides, such as aspartame (the methyl ester of the aspartic  
73 acid/phenylalanine dipeptide) and neotame (a secondary amine of 3,3-dimethylbutanal and aspartame),

74 can activate T1R2/T1R3 sweet taste receptors. In the case of umami, the umami heterodimer  
75 (T1R1/T1R3) has ligands with multiple binding sites, and thus the receptor displays low specificity  
76 and can respond to a chemically diverse range of umami molecules. More than 50 peptides (such as  
77 KGDEESLA) appear to elicit umami, but their specific functional roles remain unclear. Research on  
78 the relevant receptors has suggested that such peptides might directly lead to the sensation of umami.  
79 However, it is also possible that umami is a consequence of partial hydrolysis, which leads to sizeable  
80 concentrations of Asp or Glu (Temussi, 2012; Wang et al., 2020).

81 Several experimental approaches have been used to study the sensory properties of protein fractions.  
82 The most common strategy to examine how specific compounds affect the sensory characteristics of  
83 products, using a combination of fractionation and omission tests (Engel et al., 2002; Toelstede &  
84 Hofmann, 2008). However, peptidomics techniques are increasingly used thanks to advances being  
85 made in modern mass spectrometry and bioinformatics. These tools are ideally suited for carrying out  
86 comprehensive peptide analysis, especially when such analyses exploit the massive quantities of  
87 information currently available in genomic and transcriptomic databases. In peptidomics, different  
88 solvents and techniques are used in the fractionation, separation, and analysis of peptides (Gao et al.,  
89 2019; Salger et al., 2019). In such work, liquid chromatography-mass spectrometry is the most widely  
90 used analytical method. Fragmentation spectra obtained from samples are compared with theoretically  
91 expected spectra for peptide reference sequences. Sample peptides are thus assigned to the proteins  
92 that contain their sequences. Several bioinformatics tools have been developed to automate these  
93 operations, such as COMET (Eng et al., 2013) or X!tandempipeline (Langella et al., 2017).

94 Information about peptide properties can be found in databases such as BIOPEP (Iwaniak et al., 2016).  
95 Recently, Daher et al. (2020) demonstrated that peptidomics could be a valuable tool for evaluating the  
96 bitterness of protein isolates.

97 Thus, the aim of this study was to identify the main oligopeptides and polypeptides (5–40 amino acids  
98 long) found in pea protein isolates and to characterize their sensory properties. To this end, we used  
99 pea protein solutions and an experimental design previously employed by Cosson et al. (2021). The  
100 peptide profiles of the solutions were determined using ultra high-performance liquid chromatography  
101 coupled with mass spectrometry (UHPLC-MS/MS). The resulting peptides were identified, and both

102 their physicochemical properties and their antioxidative properties were characterized. Then, we  
103 examined the impact of our fraction-based formulation strategy on peptide profile. Finally, the  
104 relationship between peptide profiles and the sensory properties of solutions (as determined in Cosson  
105 et al., 2021) was explored, with a particular focus on perceived bitterness.

106

## 107 **2. Materials and methods**

### 108 **2.1. Solution preparation**

109 To obtain a pea protein isolate, different unit fractionation steps (precipitation, centrifugation,  
110 membrane separation) followed by heat treatments are implemented. These processing steps influence  
111 sensory characteristics as well as functional property of products (Gharibzahedi & Smith, 2021;  
112 Roland *et al.*, 2017). Thus, two commercial pea protein isolates were used in this study. Six fractions  
113 were obtained from two pea protein isolates (protein content = nitrogen [N] content x 6.25; 83% dry  
114 matter) as explained in Cosson et al. (2021): permeates a and b; retentates a and b; and pellets a and b.  
115 The main elements of fractionation are recalled here. The isolates were dispersed in tap water to obtain  
116 a suspension (4% (w/w) dry matter content) and maintained under agitation for 12 h at 3 °C. Then, it  
117 was centrifuged (Jouan Kr4i and a Sorvall Lynx 4000 [Thermo Scientific, Waltham, US]; 6000 g, 10  
118 min, 4 °C) and the supernatant was manually separated from the pellet. The pellet was then diluted  
119 with tap water (12.35% (w/w) dry matter content). Then, a tangential filtration module (TIA, Bollene,  
120 France) was used with two ST-3B-1812 PES Synder membranes (46-mil spacer; 10-kDa MWCO) and  
121 a high-pressure diaphragm pump (Wanner Hydra-Cell G10, Wanner International Ltd, Church  
122 Crookham, UK). Throughout filtration, the retentate was at 13 °C, the inlet pressure (P1) was at 1.5  
123 bar, the outlet retentate pressure (P2) was at 1 bar, and the mean transmembrane pressure ( $(P1 + P2)/2$ )  
124 was at 1.25 bar. First, ultrafiltration was used to obtain 10 L of permeate; then, diafiltration was  
125 performed to partially wash the retentate with one diavolume.  
126 Then, these six fractions were combined in various ways to formulate the 28 unique and different  
127 solutions of the mixture design described in Cosson et al., 2021 (see Supplementary Table 1). Among  
128 these solutions Refa (respectively Refb) correspond to the solutions of pea protein isolates a (resp. b)  
129 at 4% (w/w). This process was carried out at 4°C in 50 mL glass flasks, which were stored at -20°C.

130 Work was performed on different groups of compound types rather than on a single compound type.  
131 Each fraction was associated with a main compound type: insoluble proteins in the case of the pellets;  
132 soluble compounds (e.g., volatiles, peptides, and phenolics) in the case of the permeates; and soluble  
133 proteins interacting with volatiles in the case of the retentates. This approach made it possible to  
134 formulate a diversity of pea-protein-based solutions to obtain continuous responses and build reliable  
135 statistical models. Solutions were chosen to represent a broad spectrum of combinations while also  
136 remaining realistic in terms of protein concentrations (0–4.25%). The different steps to obtain the  
137 solutions and the solutions analysis are described in the Supplementary Figure 1.

138

## 139 **2.2. Overall characterization of the solutions**

140 For each fraction, protein content was determined via the Kjeldahl method (N content x 6.25). Dry  
141 matter content (% w/w) and ash content were determined by a certified external laboratory (SAS  
142 IMPROVE, Amiens, France) via drying and calcination (prepASH<sup>®</sup> 219 analysis system). Conductivity  
143 at 20°C was measured with a calibrated conductivity probe (InPro 7108-25/65-VP 3.B, M300  
144 transmitters; Mettler Toledo, Switzerland), and pH was measured at 20°C (InPro 4801i/SG/120;  
145 Mettler Toledo, Switzerland).

146 Hydrophobicity index values were measured as per Kato and Nakai (1980). The reaction between the  
147 8-anilinonaphthalene-1-sulphonic acid probe (ANS) and hydrophobic amino acids (Alanine, Valine,  
148 Leucine, Isoleucine, Methionine, Phenylalanine, Tryptophan, Proline) leads to the formation of a  
149 fluorescent complex, which is measured by spectrofluorometry. Each solution was diluted with  
150 phosphate buffer (0.053 M Na<sub>2</sub>HPO<sub>4</sub>-2H<sub>2</sub>O, 0.067 M KH<sub>2</sub>PO<sub>4</sub>, pH = 7.0) to establish five  
151 concentration levels between 0.002% and 0.032% (wt). Then, 20 µL of an 8-anilinonaphthalene-1-  
152 sulphonic acid probe (ANS; Sigma Aldrich) was added to 4 mL of each solution; the result was  
153 thoroughly mixed for 15 min in the dark (concentration of 8 mM in the phosphate buffer). Signal  
154 intensity was measured using a spectrofluorometer (Cary Eclipse; Agilent) with excitation  
155 wavelengths of 380nm and emission wavelengths of 480nm. Protein surface hydrophobicity was then  
156 calculated as the initial slope of relative fluorescent intensity in function of the protein concentration.  
157 The relative fluorescent intensity was calculated as  $(F-F_0)/F_0$  where  $F_0$  is the fluorescent intensity

158 values of the ANS blanks (ANS solution made with buffer - without any proteins). F is the fluorescent  
159 intensity values of the protein solutions. The slope of the relationship between protein concentration  
160 (%) and fluorescent intensity was determined via linear regression analysis. Three replicates of the  
161 analysis were performed.

162

### 163 **2.3. Peptide identification and relative quantification**

164 Before the UHPLC-MS/MS analysis, a sample pre-treatment procedure was applied adapted from  
165 previous work (Guillot et al., 2016). Due to the nature of the samples, which are the result of several  
166 fractionation steps, it was possible to simplify the sample preparation procedure as follows. Pea  
167 solutions were centrifuged (15,000 g, 4°C, 15 min). The supernatants were filtered using a Vivaspin  
168 centrifugal concentrator (20 mL, 10 kDa; Sigma Aldrich) run at 8,000 g (30 min, 4°C). The filtrates  
169 were stored in the dark at -80°C prior to analysis.

170 MS was performed at the PAPPSO platform (MICALIS, INRAE, Jouy-en-Josas, France). An Orbitrap  
171 Fusion™ Lumos™ Tribrid™ mass spectrometer (Thermo Fisher Scientific) coupled to an UltiMate™  
172 3000 RSLCnano System (Thermo Fisher Scientific) was used. Peptides were loaded into a precolumn  
173 (Acclaim PepMap C18; 5 µm particle size, 5 mm length, 300 µm ID) at a rate of 20 µL/min and were  
174 separated using a C18 column (Acclaim PepMap nanoViper; 2 µm particle size, 500 mm length, 75  
175 µm ID) at a rate of 300 nl/min and measured over a total gradient length of 147 min with increasing  
176 buffer B (80% acetonitrile [ACN] and 0.1% formic acid) from 1 to 60 % for 115 min. Buffer A was  
177 0,1% formic acid in 98% water. The eluted peptides were distributed throughout the gradient showing  
178 a good and an adequate peptide separation (Supplementary Figure 2). The eluted peptides were  
179 analyzed online using the Orbitrap mass analyzer. The mass spectrometer was operated in data  
180 dependent acquisition (DDA) and positive mode ionization was performed, employing a spray voltage  
181 of 2.8 kV. Peptide ions were analyzed using a data-dependent method as follows: a full MS scan (m/z:  
182 300–1,600; resolution: 120,000) was performed by the Orbitrap mass analyzer. Doubly and triply  
183 charged peptides underwent MS/MS analysis (collision energy: 30%; resolution: 30,000; cycle time: 3  
184 sec).

185 Peptide identification was performed with X!Tandem v. 2017.2.14 (Alanine) and X!Tandem Pipeline  
186 (C++) v. 0.2.40 (Langella et al., 2017) using protein sequences for *Pisum sativum* L. The main peptide  
187 identification parameters were the following: no cleavage specificity, variable methionine oxidation  
188 state, and mass tolerance for parent and fragment ions of  $\pm 10$  ppm. Peptides were retained when the E-  
189 value was  $\leq 0.05$ , and the presence of one peptide per parental protein was considered to enable  
190 identification. Contaminant peptides were discarded following identification using a standard  
191 proteomics contaminant database, and the false discovery rate was estimated using the reversed  
192 protein database.

193 MassChroQ software (v. 2.2.17) was employed to perform alignment, XIC extraction, peak detection,  
194 and quantification (Valot et al., 2011).

195 Fourteen pea solutions were analyzed using UHPLC-MS/MS: Refa, Refb, 100Pa, 100Pb, 100Ra,  
196 100Rb, 50Ia-50W, 50Ib-50W, 50Pb-25Ib-25W, 25Pa-25Ra-13Ia-38W, 70Pb-30Ra, 40Ra-30Ib-30W,  
197 50Ra-25Ia-25W, and 50Pb-50Rb. Among them, 100Ra, 100Rb, Refa, and Refb were performed in  
198 duplicate to assess method repeatability.

199 To cut down on the analysis time, we hypothesized that the solutions' peptide concentrations could be  
200 estimated from solution formulations, given that the solutions were mixtures of the fractions. We  
201 found support for this hypothesis using a subset of six of the solutions (50Pb-25Ib-25W, 25Pa-25Ra-  
202 13Ia-38W, 70Pb-30Ra, 40Ra-30Ib-30W, 50Ra-25Ia-25W, and 50Pb-50Rb). For the other thirteen  
203 solutions (50Pa-Ia25-W25, 50Rb-50W, 40Pb-60W, 50Pb-50W, 40Pa-60Rb, 30Ia-70W, 60Ra-40W,  
204 50Pa-25Ib-25W, 40Pa-60W, 50Pa-50Ra, 40Rb-30Ia-30W, 25Ib-75W, and 40Rb-30Ib-30W), peptide  
205 composition was calculated based on the peptide composition of the fractions. A linear equation of the  
206 following type was used:

$$207 \quad A_{\text{Recombined.Products}} = A_{\text{pellet.a}} \times C_{\text{pellet.a}} + A_{\text{retentate.a}} \times C_{\text{retentate.a}} + A_{\text{permeate.a}} \times C_{\text{permeate.a}} + A_{\text{pellet.b}} \times C_{\text{pellet.b}} + \\ 208 \quad A_{\text{retentate.b}} \times C_{\text{retentate.b}} + A_{\text{permeate.b}} \times C_{\text{permeate.b}}$$

209 where A was the area of the peptides, and C was the relative quantity of each fraction.

210 Before the statistical analyses were performed, the data were processed. First, the areas of each  
211 replicate were averaged (cleansing step). The areas of identical peptides with the same charges were  
212 also summed. In this study, we chose to use all a peptide's isotopes in its quantification. This decision

213 was made for two reasons: a) the isotope distribution for a given peptide is discrete and depends  
214 mainly on the presence of heavy isotopes and b) isotope composition can be treated as  
215 "homogeneous." Consequently, using all the isotope peaks should improve the results because signal  
216 variability should decline if multiple values are used. Missing data are always a modeling concern, so  
217 we assumed that this approach would still yield a better approximation than comparing isotopes  
218 separately. Second, certain peptides were removed (first filtering step): only peptides present in at least  
219 two solutions were retained. Third, the peptide composition of 13 of the solutions was calculated as  
220 described above (calculation step). Fourth, peptides with little variation in area were removed (second  
221 filtering step): only peptides that varied at least 50% among the solutions were retained. Finally, to  
222 remove any artefacts, null values were replaced by randomly selected values between  $1+E04$  and  
223  $1+E05$  (i.e., values corresponding to the detection threshold). The general workflow of the different  
224 steps of peptidomics analysis is illustrated below (Fig. 1).

225

#### 226 **2.4. Characterization of peptide properties**

227 Peptides were characterized based on nine physicochemical properties: length (number of amino  
228 acids), the GRAVY index (the grand average of hydrophobicity), bulk (the average bulkiness of the  
229 amino acids), the aliphatic index (relative volume occupied by aliphatic side chains), polarity (average  
230 polarity of the amino acids), charge (overall net charge), relative basic nature (fraction of informative  
231 positions that are occupied by Arg, His, or Lys), relative acidic nature (fraction of informative  
232 positions that are occupied by Asp or Glu), and relative aromatic nature (fraction of informative  
233 positions that are occupied by His, Phe, Trp, or Tyr). As in Proust et al. (2019), these properties were  
234 computed using the aminoAcidProperties function of the R package "alakazam" v. 0.2.8 (Gupta et al.,  
235 2015). Default settings were used for scaling and normalization. The bioactivity and sensory  
236 properties of peptides were explored via comparisons with known bioactive and taste peptides listed in  
237 the BIOPEP database (Iwaniak et al., 2016). Only peptides that were more than three amino acids long  
238 were examined to avoid noise in the results. Finally, the perceptions of peptides were investigated by  
239 looking at the sensory scores of the 28 solutions evaluated by Cosson et al. (2021).

240

## 241 **2.5. Statistical analysis**

242 Analyses were performed using R (R Core Team, 2019) and JMP (v. 13.1.0; SAS Institute Inc., Cary,  
243 SC, USA). For the inferential analyses,  $\alpha = 0.05$  was the threshold for statistical significance. To  
244 visualize the intersections in the peptide sets among the six fractions and the two raw solutions, the  
245 function “upset” in the package UpSetR was used (Conway et al., 2017). To visually explore  
246 differences in peptide profiles among the 28 solutions, we carried out principal component analysis  
247 (PCA, wide method) on a correlation matrix. To visualize the overall characteristics of the peptides,  
248 we plotted the distributions of each physicochemical property (normalized distribution, kernel  
249 density). Finally, to examine the relationships between the peptide data and the sensory data for the 28  
250 solutions, we analyzed a correlation matrix (Pearson method).

251

## 252 **3. Results and discussion**

### 253 **3.1. Identification and characterization of the main peptides in pea protein isolate solutions**

#### 254 *3.1.1. Identification of the peptides in the pea protein solutions*

255 After preliminary processing of the peptide data, 3,561 peptide ions (with different charges) and 3,005  
256 unique peptides were identified. Mass ions varied in  $m/z$  (305–1395  $m/z$ ), charge (2–4), isotope  
257 number (0–5), and area ( $1.0E+04$ – $1.0E+10$ , median =  $1.4E+06$ ). The three most common peptides  
258 were NPFIFK, FANAQPQQR, and NQKQSYF; they came from vicilins and provicilins. They likely  
259 represent favored hydrolysis sites. In addition, 348 peptides with the following modifications were  
260 identified: loss of an ammonia, usually via vicinal dehydration, ammonia rearrangement, and  
261 rehydration via ammonia release, resulting in the loss of nitrogen without any gain in oxygen  
262 (MOD:01160); oxygenation of an L-methionine residue to form a diastereomeric L-methionine  
263 sulfoxide residue (MOD:00719); replacement of a residue amino or amino hydrogen with an acetyl  
264 group (MOD:00408); and formation of a double bond via the removal of a water molecule from a  
265 residue (MOD:00704) (Jupp et al., 2015).

266 The 3,005 peptides had origins in a wide range of proteins from three main groups (Fig. 2): storage  
267 proteins (45%), enzymes (23%), and proteins derived from seed metabolism (32%). Within these

268 groups, only the proteins with the most peptides are illustrated. The others have been grouped  
269 according to their functions. The majority of the peptides came from storage proteins and more  
270 specifically, from vicilins (18%), convicilins (4%), and legumins (11%). This result is not surprising  
271 since protein isolates are mainly composed of the latter three protein types (Crevieu-Gabriel, 1999).  
272 It was interesting to note the presence of peptides from proteins associated with sensory off-notes.  
273 There were large quantities of peptides from lipoxygenases (7%), which catalyze the degradation of  
274 polyunsaturated fatty acids; the latter are thought to play an important role in the development of  
275 undesirable off-flavors in pulses. The initial products of lipoxygenase activity are hydroperoxides,  
276 which are further degraded into a wide range of compounds, including many that are responsible for  
277 off-flavors, such as hexanal and n-pentylfuran (Roland et al., 2017). In addition, peptides from  
278 aldehyde dehydrogenase were observed. This enzyme catalyzes the oxidation of aldehydes and so can  
279 modify the composition of volatile compounds of pea protein solutions and so the sensations of  
280 beaniness. Peptides from protein that catalyzes phenolic acids modifications were observed:  
281 carotenoid cleavage dioxygenase, chalcone synthase, gibberellin dioxygenase, and isoflavone synthase  
282 were present. Phenolics acids play also a role in the development of undesirable off-flavors in pulse  
283 (bitter and astringent notes).

284 The peptides displaying modifications were generally associated with three types of proteins:  
285 lipoxygenases (10% of modified peptides), histones (12% of modified peptides), and ribosomal  
286 proteins (5% of modified peptides). Peptides from these protein types could probably more sensitive to  
287 modifications during the pea processing.

288 Thus, these results show that a wide variety of peptides were identified. These peptides represent  
289 proteins from different families, mainly seed storage proteins. Clarifying the origin of these peptides  
290 also gives us information about the proteins present in the isolates, including which proteins may  
291 cause sensory perceptions (e.g., the lipoxygenases).

292

### 293 *3.1.2. Physicochemical properties of the peptides in the pea protein solutions*

294 The peptides' physicochemical and antioxidative properties were characterized. The nine  
295 physicochemical properties were chosen with a view to comprehensively describing pea peptide

296 diversity. The normalized distributions of the property values for the peptides are in Figure 3. The  
297 peptides were mostly polar and hydrophilic. The mean GRAVY index value was around -0.5, which is  
298 also the overall mean value for the 20 standard amino acids (i.e., -0.49; Kyte & Doolittle, 1982). The  
299 median net charge was close to zero. Mean bulk was around 15 Å, which is also the overall mean for  
300 the 20 standard amino acids (i.e., 15.4 Å; Zimmerman et al., 1968). In terms of amino acid  
301 composition, the peptides had more aliphatic amino acids (Ala, Val, Leu, and Ile) than aromatic amino  
302 acids (His, Phe, Trp, and Tyr) or acidic amino acids (Asp and Glu). Finally, average length was 10  
303 residues, although this observation should be interpreted with caution given the specificities of the  
304 analytical pipeline. Indeed, the upper limit on length was defined by the purification process and, more  
305 specifically, by the ultrafiltration steps; the lower limit on length (no peptides < 6 residues were  
306 detected) was a direct consequence of the chosen MS detection range (300–1,600 m/z). Thus, these  
307 results show that the main peptides in the pea protein isolates varied greatly in their physicochemical  
308 properties; however, when the overall averages were obtained, they generally corresponded to the  
309 averages for the 20 standard amino acids.

310 In addition, some of the identified peptides matched with antioxidant peptides observed in pea and  
311 included in BIOPEP database (see Supplementary Table 2). Bioactive peptides are usually 2–20 amino  
312 acids long and have molecular masses of less than 6 kDa (Sarmadi & Ismail, 2010; Sun et al., 2004).  
313 Here, eleven peptides had sequences that were homologous with those of known antioxidant peptides  
314 (BIOPEP database) previously identified in pea-protein-based solutions (Iwaniak et al., 2016): ADGF;  
315 ADVFNPR; ELLI; FVPH; HLHP; KFPE; LPILR; SAEHGSLH; SGAF; YLKT; and YVGD. These  
316 peptides contained many copies of phenylalanine, an amino acid known to mediate antioxidant activity  
317 (Sarmadi & Ismail, 2010). They came from different proteins—storage proteins such as legumins;  
318 enzymes such as seed linoleate 9S-lipoxygenase-3; and metabolic proteins such as transporters. These  
319 results highlight that the diversity of peptides present in pea-protein-based solutions may have  
320 nutritional benefits and could be used to enhance the value of plant-based foods. Peptide composition  
321 should be studied further from a nutritional point of view.

322

## 323 **3.2. Impact of fractionation and recombination on peptide profiles**

### 324 *3.2.1. Impact of fractionation on peptide profiles*

325 This study adopted an original approach: the decision was made to work with fractions instead of  
326 compounds because i) we had no a priori hypothesis on which compounds would be linked to  
327 perceptions and ii) from a sensory point of view working with all compounds (e.g. with molecular  
328 fractionation and omission tests) can be very long and difficult. We broke down the pea protein  
329 isolates into six fractions (two pellets, two retentates, and two permeates), which were then  
330 recombined to form different solutions using a mixture design. Before studying the recombined  
331 solutions, we studied the impact of fractionation on peptide profile composition.

332 The overall characteristics of the six fractions and the two raw solutions are presented in Table 1. The  
333 number of peptides per fraction was linearly correlated with the sum of the areas of the peptides  
334 (Pearson method;  $R^2 = 0.83$ ). The permeates (100Pa and 100Pb) contained the greatest number of  
335 peptides, followed by the raw solutions (Refa and Refb). The pellets (50Ia-50w and 50Ib-50W) had  
336 the lowest number of peptides. Solutions from pea protein isolate b (Refb, retentate 100Rb, permeate  
337 100Pb and pellet 50Ib-50W) had fewer identified peptides overall than solutions from pea protein  
338 isolate a (Refa, retentate 100Ra, permeate 100Pa and pellet 50Ia-50W). These differences could come  
339 from the processing of the two commercial products. A perspective to this work could be to study and  
340 identify the step (or steps) of the processing that generates these differences in peptide composition.

341 To visualize the intersections in peptide sets among the six fractions and the two raw solutions (Rfa  
342 and Refb), an UpSet plot was used (Fig. 4). An higher number of peptides were observed in solutions  
343 from Refa (permeate 100Pa, retentate 100Ra, refa and then pellet 50Ia-50W) than in the respective  
344 products from Refb (permeate 100Pb, retentate 100Rb, refb and pellet b). However, there were more  
345 peptides in the raw solution from Refb than in the raw solution from Refa. Thus, the two pea protein  
346 isolates were not impacted in the same way by the pea processing: it would appear that more specific  
347 peptides were “lost” from isolate b.

348 To understand the effect of fractionation on the peptide profiles of the fractions, we examined the  
349 relationship between the fractions’ physical characteristics (Table 1) and the sum of the areas of the  
350 peptides. There was not a significant correlation between peptide area and either dry matter content,

351 protein content, ash content, pH, or surface hydrophobicity. However, there was a significant linear  
352 correlation with conductivity (Pearson method;  $R^2 = 0.84$ ). Peptides (e.g., salts, which drive  
353 conductivity) are rather soluble and small in size. During the centrifugation step, they must have  
354 mostly gone into the supernatant, and then, during the filtration step, they must have passed into the  
355 permeate. Protein content and conductivity were slightly higher in isolate a than in isolate b. It can be  
356 assumed that these properties explain the higher peptide concentrations in the fractions from batch a.  
357 The peptides' physicochemical properties showed similar normalized distributions across fractions  
358 (Fig. 3). The only notable differences occurred in charge between the pellets (50Ib-50W and 50Ia-  
359 50W) and the permeates (100Pb and 100Pb) and in the polarity between the raw solutions (Refa versus  
360 Refb). The peptides in the permeate solutions varied slightly more in charge. The peptides in the raw  
361 solution Refb were slightly more polar. Therefore, the fractionation process did not lead to peptide  
362 profiles that differed in physicochemical properties. As for the eleven peptides with sequences  
363 homologous with those of known antioxidant peptides, they occurred across the range of solutions.  
364 They were, however, most common in the raw solutions (Refa and Refb).

### 365 *3.2.2. Peptide profiles of the recombined solutions*

366 A mixture design was used to create a suite of solutions by combining the pea protein fractions in  
367 different ways. To validate this methodology, the peptide profiles of six of the recombined solutions  
368 (50Pb-25Ib-25W, 25Pa-25Ra-13Ia-38W, 70Pb-30Ra, 40Ra-30Ib-30W, 50Ra-25Ia-25W, and 50Pb-  
369 50Rb) were determined; the results were compared with the peptide profiles that were calculated using  
370 the fraction-based approach. Considering the number of values to be compared (3,561 peptides x 6  
371 solutions), we did not contrast the individual values of the recombined solutions but rather the  
372 distributions of the differences between their measured and calculated values. These distributions were  
373 compared to the distributions for replicates of the experimental replicate solutions (100Ra, 100Rb,  
374 Refa and Refb). The quartiles were calculated excluding any null values. The quartiles for repeated  
375 solutions were: 1st quartile— $4.39E+05$ , median— $1.18E+06$ , 3rd quartile— $2.39E+06$ , and  
376 maximum— $6.11E+08$ . The differences between the quartiles for the measured versus calculated  
377 values were as follows: 1st quartile— $7.19E+05$ , median— $1.65E+06$ , 3rd quartile— $4.22E+06$ , and  
378 maximum— $1.47E+09$ . The overall distributions were similar between replicate solutions and the data

379 for the recombined solutions. The quartiles were slightly lower in the case of the former, but the orders  
380 of magnitude were similar. In the case of some peptides, there were significant differences between the  
381 measured and calculated values for the recombined solutions. However, these peptides were among  
382 those with the largest areas, and the relative differences were therefore small. In conclusion, it  
383 appeared that peptide profiles could be reliably estimated for the recombined solutions using fraction-  
384 based calculations.

385 PCA was used to visually assess the main differences among the recombined solutions (Fig. 5). The  
386 solutions were well distributed along axes F1 and F2, which accounted for 71.8% of the variance.  
387 Thus, the maps based on the first two axes seemed to provide a good-quality projection of the initial  
388 multidimensional table, even though some information might have remained hidden in the subsequent  
389 axes. The data for the areas of the 3,561 peptides were clustered within one half of the correlation  
390 circles and were thus clearly correlated. Overall, peptide concentrations increased from water solution  
391 (X, lower left) to the more permeate-based solutions (100 Pb and 100Pa; X upper/right). The solutions  
392 formulated with fractions from batch a (Fig. 5: in green) and the solutions formulated with fractions  
393 from batch b (Fig. 5: in blue) stand out clearly. Batch a variability is mainly found on axis 1, and batch  
394 b variability is mainly found on axis 2. Solutions formulated with fractions from both batch a and b are  
395 in the middle (Fig. 5: in orange). Regardless of the batch, permeates (100Pa and 100Pb) had the  
396 highest peptide concentrations. The pellets (50Ia-50W and 50Ib-50W) had the lowest peptide  
397 concentrations. The raw solutions (Refa and Refb) had intermediate peptide concentrations.  
398 Consequently, with this experimental design, we have managed to create two different ranges of  
399 peptide concentrations. The peptides in fraction mixtures (batch a and batch b) allowed us to explore  
400 any interactions.

### 401 **3.3. Identifying factors influencing perceived bitterness**

#### 402 *3.3.1. Sensory properties of the recombined solutions*

403 The 6 different fractions were combined in various ways to formulate 28 pea protein solutions (see  
404 Supplementary Table 1). These solutions had been used by Cosson *et al.*, in a previous sensory study  
405 to obtain greater insight into the origin of perceived beaniness (expressed via the following attributes:  
406 almond, broth, cereals, nuts, pea, and potato), bitterness, and astringency in pea-protein-based foods.

407 Cosson *et al.*, found that the attributes contributing to perceived beaniness were mainly influenced by  
408 the retentate and permeate fractions, likely because of their levels of volatiles, which were indirectly  
409 reflected by hexanal levels. Perceived astringency was mainly influenced by the retentate and pellet  
410 fractions, while perceived bitterness was largely driven by the retentate fraction. Bitterness and  
411 astringency were associated with the levels of phenolics, which were indirectly reflected by caffeic  
412 acid content. However, this previous study concluded that a more detailed analysis of solution  
413 composition (i.e., beyond hexanal and caffeic acid levels) would be needed to uncover the more  
414 precise origins of these sensory perceptions (Cosson *et al.*, 2021).

415 Drawing upon the results of this previous study, the peptide profiles of the pea protein solutions were  
416 examined in tandem with the sensory profile data. The correlations between peptide areas and sensory  
417 scores were evaluated (Pearson method). Each sensory attribute (score out of 10) was correlated with  
418 the areas of several peptides (p-value < 0.05). Correlations were most common for the broth attribute  
419 (1,640 out of 3,561 peptides), followed by the salty attribute (1,277 out of 3,561 peptides). In contrast,  
420 correlations with other attributes were significantly less frequent: bitter—275 peptides; astringent—  
421 173 peptides, mouthfeel—410 peptides, pea—440 peptides, potato—246 peptides, almond—80  
422 peptides, nuts—135 peptides, and cereals—214 peptides. We also compared the peptides from this  
423 study with the sensory peptides listed in the BIOPEP database (Iwaniak *et al.*, 2016), but there were no  
424 noteworthy findings.

425 Perceived saltiness can arise from the presence of peptides with charged terminals and/or charged side  
426 chains (Temussi, 2012). However, the phenomenon can also have an indirect cause: NaCl and peptides  
427 (small soluble molecules) are likely distributed in a similar way in pea protein fractions. Furthermore,  
428 a higher salt concentration can also change how protein hydrolysis or peptide fractionation plays out,  
429 resulting in different peptide concentrations (Cheison & Kulozik, 2017).

430 Broth notes may be perceived when peptides have activated T1R1/T1R3 umami receptors. Indeed,  
431 umami is often described as a meaty, broth-like, or savory taste and can participate in perceived  
432 brothiness (Lioe *et al.*, 2010). Such peptides are between 2 and 11 residues long. For example, Glu-  
433 Gly-Ser-Glu-Ala-Pro-Asp-Gly-Ser-Ser-Arg was found to elicit the sensation of umami during the  
434 consumption of peanut hydrolysate (Su *et al.*, 2012). However, the idea that some peptides activate

435 umami receptors is controversial because when such peptides are synthesized, they do not always elicit  
436 umami (Maehashi et al., 1999). Another explanation could be that the sensation of umami is a  
437 consequence of the peptides' partial hydrolysis, which results in sizeable concentrations of Asp or Glu  
438 (Temussi, 2012; Wang et al., 2020). Considering the number of peptides associated with the broth note  
439 (36% of the peptides), several mechanisms are likely at work. In any case, peptides appear to play a  
440 major role in the construction of brothiness.

441

### 442 *3.3.2. Relationships between peptide presence and bitterness*

443 Although bitterness is correlated with a much smaller number of peptides, it is important to discuss  
444 this sensation as well. Indeed, the bitterness of pea-protein-based foods is a major off-note in these  
445 products (Roland et al., 2017). Here, among the 275 peptides correlated with bitterness, 106 were  
446 exclusively correlated with bitterness. Many peptides have the ability to activate bitter receptors  
447 (Aubes-Dufau et al., 1995). Based on past research, such peptides are between 5 and 8 residues long  
448 (Aubes-Dufau et al., 1995; Maehashi & Huang, 2009). Here, however, only 14 of the peptides  
449 associated with bitterness were less than 8 residues in length: SRNPIY, KRHGEW, NLQNYR,  
450 SNKFGKF, NQKQSYF, YLKGLKF, YQKSTEL, APHWNIN, AQPLQRE, ISLNKIRL,  
451 NQKQSYFA, ANAQPLQR, NAQPLQRE, and EVLSWSFH. The peptides KRHGEW, NQKQSYF,  
452 NAQPLQRE, and AQPLQRE are particularly noteworthy because they were positively correlated  
453 with the bitterest solutions. In contrast, the peptides YLKGLKF, YQKSTEL, and EVLSWSFH were  
454 negatively correlated with bitterness. The correlations are shown on the Supplementary Figure 3.  
455 Using BitterX software (Huang et al., 2016), it was found that these eight peptides were highly likely  
456 to activate bitter receptors (either TA2R7 or T2R40; probability: 88–79%). However, to confirm that  
457 these peptides contribute to perceived bitterness in the mouth, it would be necessary to study their  
458 effects on bitter receptors *in vitro* or to have a sensory panel evaluate them in solution. It would also  
459 be useful to assess their concentrations relative to their perception thresholds. For example, Toelstede  
460 and Hofmann (2008) found that 12 peptides eliciting bitter sensations had recognition thresholds  
461 between 0.05 and 6.0 mmol/L.

462 In addition, while other groups of peptides correlated with sensory perceptions had largely overlapping  
463 characteristics, bitterness-related peptides displayed certain differences (Fig. 3), such as lower  
464 GRAVY values (i.e., are more hydrophilic on average), lower aliphatic values (i.e., have smaller  
465 relative volumes on average), and higher polarity (i.e., are more polar on average). These results do  
466 not concur with the results of previous studies, which have shown that such peptides are mainly  
467 hydrophobic (Kim et al., 2008). In conclusion, these peptides may affect sensations of bitterness in the  
468 mouth by activating bitter receptors (i.e., the peptides displaying positive correlations), blocking bitter  
469 receptors (i.e., the peptides displaying negative correlations), or interacting with other molecules that  
470 do either (i.e., the peptides displaying positive or negative correlations).

471

#### 472 **4. Conclusion**

473 In this study, we identified and characterized the main oligopeptides and polypeptides (5–40 amino  
474 acids long) found in pea protein solutions. We had four main findings. First, we identified a wide  
475 variety of peptides representing a range of protein families, mainly those containing seed storage  
476 proteins but also those containing proteins that can play a role in sensory perceptions, such as  
477 lipoxygenases. Second, these peptides were mostly polar and hydrophilic, and our fraction-based  
478 formulation strategy did not affect their overall physicochemical properties. Third, eleven peptides had  
479 sequences homologous with those of known antioxidant peptides. These results indicate that the  
480 variety of peptides present in pea protein solutions can have nutritional benefits. Fourth, most of the  
481 peptides in the pea protein solutions were correlated with sensory attributes. In particular, many  
482 peptides were correlated with salty and broth attributes, perhaps expressing the relationship of some  
483 peptides to umami. A lower but still significant number of peptides displayed a correlation with  
484 bitterness. These results highlight the mechanistic importance of these molecules in sensory  
485 perceptions in the mouth. Taken together, these results suggest that a better understanding of the  
486 peptide composition of plant protein isolates could help us address related sensory issues and develop  
487 plant-protein-based foods whose taste appeals more to consumers.

## 488 **5. CRediT authorship contribution statement**

489 Audrey Cosson: Methodology, Investigation, Formal analysis, Writing - Original Draft. Lydie Oliveira

490 Correia: Resources, Investigation. Nicolas Descamps: Funding acquisition. Anne Saint-Eve:

491 Methodology, Supervision, Writing - review & editing. Isabelle Souchon: Conceptualization,

492 Supervision, Writing - review & editing.

493

## 494 **6. Acknowledgments**

495 This work was funded by Roquette (Lestrem, France), the French National Research and Technology

496 Agency (ANRT-CIFRE 2017/0815), AgroParisTech (Paris, France), and the French National Research

497 Institute for Agriculture, Food, and Environment (INRAE). The authors thank the PAPPSO platform

498 (<http://pappso.inra.fr>), which is supported by INRAE (<http://www.inrae.fr>); the Ile-de-France regional

499 council (<https://www.iledefrance.fr/education-recherche>); IBiSA (<https://www.ibisa.net>); and CNRS

500 (<http://www.cnrs.fr>), which granted access to its mass spectrometry facilities. The authors also thank

501 David Forest for providing technical support.

502

## 503 **7. References**

504 Aubes-Dufau, I., Seris, J.-L., & Combes, D. (1995). Production of peptic hemoglobin hydrolyzates:

505 Bitterness demonstration and characterization. *Journal of Agricultural and Food Chemistry*, 43(8),

506 1982–1988. <https://doi.org/10.1021/jf00056a005>

507 Bi, S., Xu, X., Luo, D., Lao, F., Pang, X., Shen, Q., Hu, X., & Wu, J. (2020). Characterization of key

508 aroma compounds in raw and roasted peas (*Pisum sativum* L.) by application of instrumental and

509 sensory techniques. *Journal of Agricultural and Food Chemistry*, 68(9), 2718–2727.

510 <https://doi.org/10.1021/acs.jafc.9b07711>

511 Cheison, S. C., & Kulozik, U. (2017). Impact of the environmental conditions and substrate pre-

512 treatment on whey protein hydrolysis: A review. *Critical Reviews in Food Science and Nutrition*,

513 57(2), 418–453. <https://doi.org/10.1080/10408398.2014.959115>

514 Conway, J. R., Lex, A., & Gehlenborg, N. (2017). UpSetR: An R package for the visualization of  
515 intersecting sets and their properties. *Bioinformatics*, 33(18), 2938–2940.  
516 <https://doi.org/10.1093/bioinformatics/btx364>

517 Cosson, A., Blumenthal, D., Descamps, N., Souchon, I., & Saint-Eve, A. (2021). Using a mixture  
518 design and fraction-based formulation to better understand perceptions of plant-protein-based  
519 solutions. *Food Research International*, 110151. <https://doi.org/10.1016/j.foodres.2021.110151>

520 Crevieu-Gabriel, I. (1999). Digestion des protéines végétales chez les monogastriques. Exemple  
521 des protéines de pois. *INRA Prod. Anim.*, 12 (2), 147-161.

522 Daher, D., Deracinois, B., Baniel, A., Watez, E., Dantin, J., Froidevaux, R., Chollet, S., & Flahaut, C.  
523 (2020). Principal component analysis from mass spectrometry data combined to a sensory evaluation  
524 as a suitable method for assessing bitterness of enzymatic hydrolysates produced from micellar casein  
525 proteins. *Foods*, 9(10), 1354. <https://doi.org/10.3390/foods9101354>

526 Davis, J., Sonesson, U., Baumgartner, D. U., & Nemecek, T. (2010). Environmental impact of four  
527 meals with different protein sources: Case studies in Spain and Sweden. *Food Research International*,  
528 43(7), 1874–1884. <https://doi.org/10.1016/j.foodres.2009.08.017>

529 Eng, J. K., Jahan, T. A., & Hoopmann, M. R. (2013). Comet: An open-source MS/MS sequence  
530 database search tool. *Proteomics*, 13(1), 22–24. <https://doi.org/10.1002/pmic.201200439>

531 Engel, E., Nicklaus, S., Salles, C., & Le Quéré, J.-L. (2002). Relevance of omission tests to determine  
532 flavour-active compounds in food: Application to cheese taste. *Food Quality and Preference*, 13(7),  
533 505–513. [https://doi.org/10.1016/S0950-3293\(02\)00136-2](https://doi.org/10.1016/S0950-3293(02)00136-2)

534 Gao, Q., Jiang, H., Tang, F., Cao, H., Wu, X., Qi, F., Sun, J., & Yang, J. (2019). Evaluation of the  
535 bitter components of bamboo shoots using a metabolomics approach. *Food & Function*, 10(1), 90–98.  
536 <https://doi.org/10.1039/C8FO01820K>

537 Gupta, N. T., Vander Heiden, J. A., Uduman, M., Gadala-Maria, D., Yaari, G., & Kleinstein, S. H.  
538 (2015). Change-O: A toolkit for analyzing large-scale B cell immunoglobulin repertoire sequencing  
539 data: Table 1. *Bioinformatics*, 31(20), 3356–3358. <https://doi.org/10.1093/bioinformatics/btv359>

540 Heng, L., Vincken, J.-P., van Koningsveld, G., Legger, A., Gruppen, H., van Boekel, T., Roozen, J., &  
541 Voragen, F. (2006). Bitterness of saponins and their content in dry peas. *Journal of the Science of*  
542 *Food and Agriculture*, 86(8), 1225–1231. <https://doi.org/10.1002/jsfa.2473>  
543 Huang, W., Shen, Q., Su, X., Ji, M., Liu, X., Chen, Y., Lu, S., Zhuang, H., & Zhang, J. (2016).  
544 BitterX: A tool for understanding bitter taste in humans. *Scientific Reports*, 6(1), 23450.  
545 <https://doi.org/10.1038/srep23450>  
546 Gharibzahedi, S. M. T., & Smith, B. (2021). Effects of high hydrostatic pressure on the quality and  
547 functionality of protein isolates, concentrates, and hydrolysates derived from pulse legumes: A review.  
548 *Trends in Food Science & Technology*, 107, 466–479. <https://doi.org/10.1016/j.tifs.2020.11.016>  
549 Guillot, A., Boulay, M., Chambellon, É., Gitton, C., Monnet, V., & Juillard, V. (2016). Mass  
550 spectrometry analysis of the extracellular peptidome of *Lactococcus lactis*: Lines of evidence for the  
551 coexistence of extracellular protein hydrolysis and intracellular peptide excretion. *Journal of Proteome*  
552 *Research*, 15(9), 3214–3224. <https://doi.org/10.1021/acs.jproteome.6b00424>  
553 Iwaniak, A., Minkiewicz, P., Darewicz, M., Sieniawski, K., & Starowicz, P. (2016). BIOPEP database  
554 of sensory peptides and amino acids. *Food Research International*, 85, 155–161.  
555 <https://doi.org/10.1016/j.foodres.2016.04.031>  
556 Jupp, S., Burdett, T., Malone, J., Leroy, C., Pearce, M., & Parkinson, H. (2015). A new ontology  
557 lookup service at EMBL-EBI. 2. *SWAT4LS*, 118-119  
558 Kato, A., & Nakai, S. (1980). Hydrophobicity determined by a fluorescence probe method and its  
559 correlation with surface properties of proteins. *Biochimica et Biophysica Acta (BBA)-Protein*  
560 *Structure*, 624(1), 13–20. [https://doi.org/10.1016/0005-2795\(80\)90220-2](https://doi.org/10.1016/0005-2795(80)90220-2)  
561 Kim, M.-R., Yukio, K., Kim, K. M., & Lee, C.-H. (2008). Tastes and structures of bitter peptide,  
562 Asparagine-Alanine-Leucine-Proline-Glutamate, and its synthetic analogues. *Journal of Agricultural*  
563 *and Food Chemistry*, 56(14), 5852–5858. <https://doi.org/10.1021/jf7036664>  
564 Kyte, J., & Doolittle, R. F. (1982). A simple method for displaying the hydropathic character of a  
565 protein. *Journal of Molecular Biology*, 157(1), 105–132. [https://doi.org/10.1016/0022-2836\(82\)90515-](https://doi.org/10.1016/0022-2836(82)90515-0)  
566 0

567 Langella, O., Valot, B., Balliau, T., Blein-Nicolas, M., Bonhomme, L., & Zivy, M. (2017).  
568 X!TandemPipeline: A Tool to manage sequence redundancy for protein inference and phosphosite  
569 identification. *Journal of Proteome Research*, 16(2), 494–503.  
570 <https://doi.org/10.1021/acs.jproteome.6b00632>

571 Li, H., & Aluko, R. E. (2010). Identification and inhibitory properties of multifunctional peptides from  
572 pea protein hydrolysate. *Journal of Agricultural and Food Chemistry*, 58(21), 11471–11476.  
573 <https://doi.org/10.1021/jf102538g>

574 Lioe, H. N., Selamat, J., & Yasuda, M. (2010). Soy sauce and its umami taste: a link from the past to  
575 current situation. *Journal of Food Science*, 75(3), R71–R76. [https://doi.org/10.1111/j.1750-](https://doi.org/10.1111/j.1750-3841.2010.01529.x)  
576 [3841.2010.01529.x](https://doi.org/10.1111/j.1750-3841.2010.01529.x)

577 Maehashi, K., & Huang, L. (2009). Bitter peptides and bitter taste receptors. *Cellular and Molecular*  
578 *Life Sciences*, 66(10), 1661–1671. <https://doi.org/10.1007/s00018-009-8755-9>

579 Maehashi, Kenji, Matsuzaki, M., Yamamoto, Y., & Udaka, S. (1999). Isolation of peptides from an  
580 enzymatic hydrolysate of food proteins and characterization of their taste properties. *Biosci Biotechnol*  
581 *Biochem*, 63(3), 555–559. <https://doi.org/10.1271/bbb.63.555>

582 Proust, L., Sourabié, A., Pedersen, M., Besançon, I., Haudebourg, E., Monnet, V., & Juillard, V.  
583 (2019). Insights into the complexity of yeast extract peptides and their utilization by *Streptococcus*  
584 *thermophilus*. *Frontiers in Microbiology*, 10, 906. <https://doi.org/10.3389/fmicb.2019.00906>

585 Roland, W. S. U., Pouvreau, L., Curran, J., van de Velde, F., & de Kok, P. M. T. (2017). Flavor  
586 aspects of pulse ingredients. *Cereal Chemistry Journal*, 94(1), 58–65.  
587 <https://doi.org/10.1094/CCHEM-06-16-0161-FI>

588 Salger, M., Stark, T. D., & Hofmann, T. (2019). Taste modulating peptides from overfermented Cocoa  
589 Beans. *Journal of Agricultural and Food Chemistry*, 67(15), 4311–4320.  
590 <https://doi.org/10.1021/acs.jafc.9b00905>

591 Sarmadi, B. H., & Ismail, A. (2010). Antioxidative peptides from food proteins: A review. *Peptides*,  
592 31(10), 1949–1956. <https://doi.org/10.1016/j.peptides.2010.06.020>

593 Sirtori, E., Isak, I., Resta, D., Boschin, G., & Arnoldi, A. (2012). Mechanical and thermal processing  
594 effects on protein integrity and peptide fingerprint of pea protein isolate. *Food Chemistry*, 134(1),  
595 113–121. <https://doi.org/10.1016/j.foodchem.2012.02.073>

596 Su, G., Cui, C., Zheng, L., Yang, B., Ren, J., & Zhao, M. (2012). Isolation and identification of two  
597 novel umami and umami-enhancing peptides from peanut hydrolysate by consecutive chromatography  
598 and MALDI-TOF/TOF MS. *Food Chemistry*, 135(2), 479–485.  
599 <https://doi.org/10.1016/j.foodchem.2012.04.130>

600 Sun, J., He, H., & Xie, B. J. (2004). Novel antioxidant peptides from fermented mushroom  
601 *Ganoderma lucidum*. *Journal of Agricultural and Food Chemistry*, 52(21), 6646–6652.  
602 <https://doi.org/10.1021/jf0495136>

603 Temussi, P. A. (2012). The good taste of peptides: peptides taste. *Journal of Peptide Science*, 18(2),  
604 73–82. <https://doi.org/10.1002/psc.1428>

605 Toelstede, S., & Hofmann, T. (2008). Sensomics mapping and identification of the key bitter  
606 metabolites in Gouda cheese. *Journal of Agricultural and Food Chemistry*, 56(8), 2795–2804.  
607 <https://doi.org/10.1021/jf7036533>

608 Valot, B., Langella, O., Nano, E., & Zivy, M. (2011). MassChroQ: A versatile tool for mass  
609 spectrometry quantification. *Proteomics*, 11, 3572–3577. <https://doi.org/10.1002/pmic.201100120>

610 Wang, W., Zhou, X., & Liu, Y. (2020). Characterization and evaluation of umami taste: A review.  
611 *Trends in Analytical Chemistry*, 127, 115876. <https://doi.org/10.1016/j.trac.2020.115876>

612 Zimmerman, J. M., Eliezer, N., & Simha, R. (1968). The characterization of amino acid sequences in  
613 proteins by statistical methods. *Journal of Theoretical Biology*, 21(2), 170–201.  
614 [https://doi.org/10.1016/0022-5193\(68\)90069-6](https://doi.org/10.1016/0022-5193(68)90069-6)

615

616 **Table 1:** Overall characteristics of the six fractions and the two raw solutions

	Number of peptides identified	Sum of peptide area	Dry matter content (% w/w)	Protein content (%)	Ash content (%)	Conductivity (mS/cm) at 20°C	pH at 20°C	Surface hydrophobicity index
<b>100Pa</b>	2586	1.31E+11	0.20	0.04	0.07	1.44	8.4	363
<b>100Pb</b>	1756	4.92E+10	0.20	0.04	0.04	1.16	9.3	298
<b>100Ra</b>	2376	7.05E+10	1.70	1.41	0.15	1.08	7.5	933
<b>100Rb</b>	1551	2.98E+10	1.70	1.48	0.12	0.88	7.5	1269
<b>50Ia-50W</b>	1565	3.72E+10	6.00	4.91	0.18	1.06	7.5	2083
<b>50Ib-50W</b>	809	9.26E+09	6.00	5.10	0.19	0.84	7.5	2172
<b>Refa</b>	2235	7.13E+10	94.00	79.05	4.14	1.09	7.5	2961
<b>Refb</b>	1488	2.26E+10	93.70	80.68	3.84	1.01	7.5	3504

617

618

619 **Captions to Figures**

620

621 **Figure 1:** General workflow of the different steps of peptidomic analysis: the preparation and  
622 measurement processes (in orange) to the bioinformatic analyses (in blue), the preprocessing of the  
623 data (in green), and the calculations for the recombined products (in yellow).

624

625 **Figure 2:** Categorization of the 3,005 unique peptides identified via UHPLC-MS/MS based on protein  
626 origin (threshold for peptide number: 24).

627

628 **Figure 3:** A) Distribution of the overall 3,561 peptides on the 28 solutions (normalized distribution,  
629 kernel density): A1 = Relative aromatic nature; A2 = Relative acidic nature; A3 = Aliphatic index; A4  
630 = Relative basic nature; A5 = Polarity; A6 = Bulk; A7 = GRAVY index; A8 = Length; A9 = Charge.

631 B) Comparison of distributions of the overall 3,561 peptides (normalized distribution, kernel density):  
632 B1 = Charge with 50Ib-50W in blue; 100Rb in green and 100Pb in red; B2 = Charge with 50Ia-50W  
633 in blue; 100Ra in green and 100Pa in red; B3 = Polarity with Refa in yellow and Refb in orange.

634 C) Comparison of distributions of the overall peptides (3,561 peptides in blue) and for the peptides  
635 correlated to bitterness (275 peptides in red) on the 28 solutions (normalized distribution, kernel  
636 density): C1 = Polarity; C2 = Aliphatic index; C3 = GRAVY index.

637

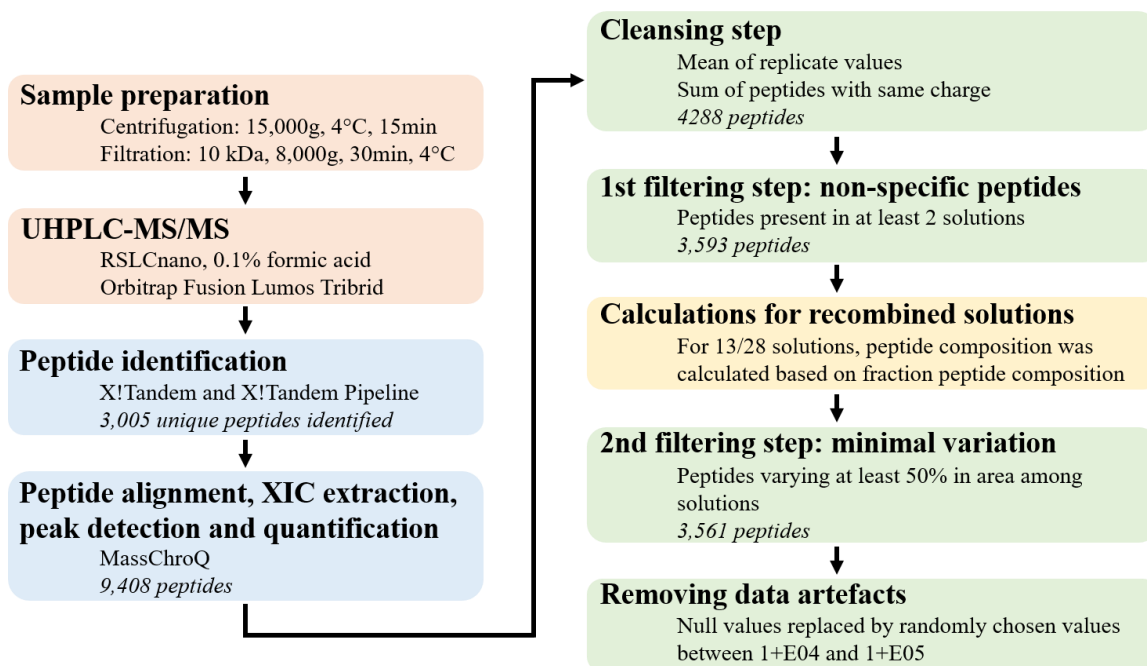
638 **Figure 4:** Depiction of the intersections in peptide sets among the six fractions and the two raw  
639 solutions (UpSet plot). The blue horizontal bars show the number of peptides in each fraction/solution.  
640 The black dots and lines show the combinations of peptides that make up each cluster or subset of the  
641 fractions/solutions. The vertical histogram shows the number of peptides in each subset.

642

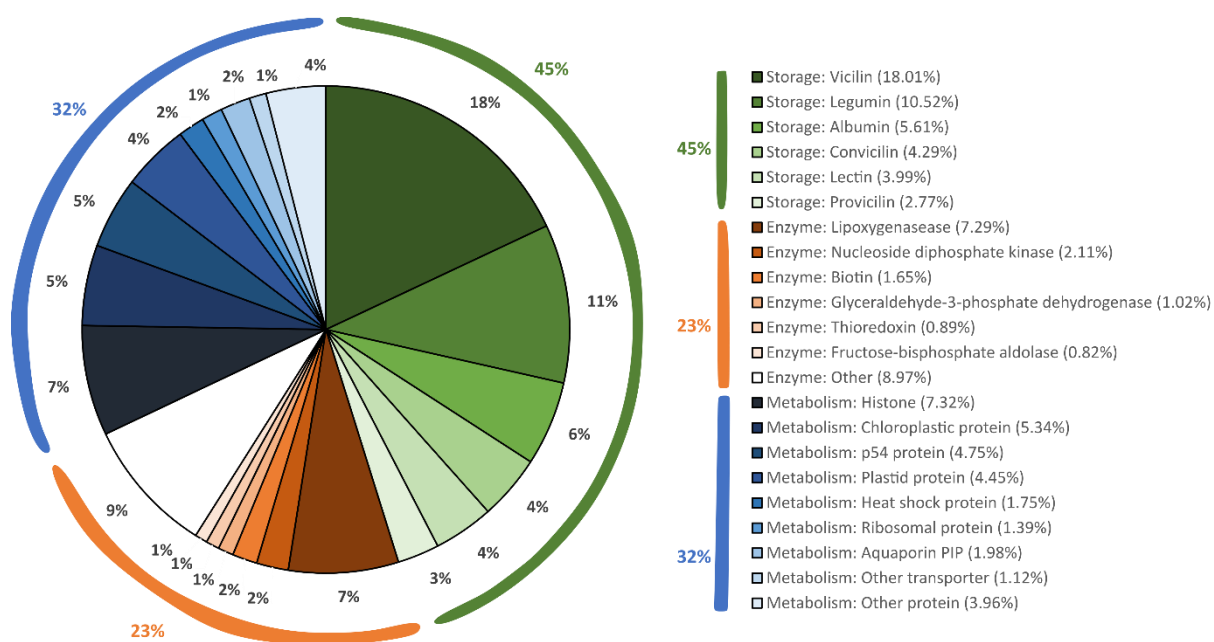
643 **Figure 5:** Results of the principal component analysis (PCA, wide method) examining the peptide  
644 profiles for the 28 solutions, which were determined using a fraction-based formulation strategy and  
645 the peptides that had been identified (based on 3,561 peptides). On the left is a loading plot showing  
646 the correlational relationships between the PCA axes 1 and 2 and the peptide areas. On the right is a  
647 PCA plot with the same two axes that shows the relative similarity in the solutions' peptide profiles.  
648 The green circles are the recombined solutions created from batch b. The blue triangles are the  
649 recombined solutions created from batch a. The orange squares are the recombined solutions created  
650 from batch a and batch b. The dark star is the water solution. The solid symbols represent the  
651 measured values, and the empty symbols represent the calculated values.

652

653 **Figure 1:** General workflow of the different steps of peptidomic analysis: the preparation and  
 654 measurement processes (in orange) to the bioinformatic analyses (in blue), the preprocessing of the  
 655 data (in green), and the calculations for the recombined products (in yellow).  
 656



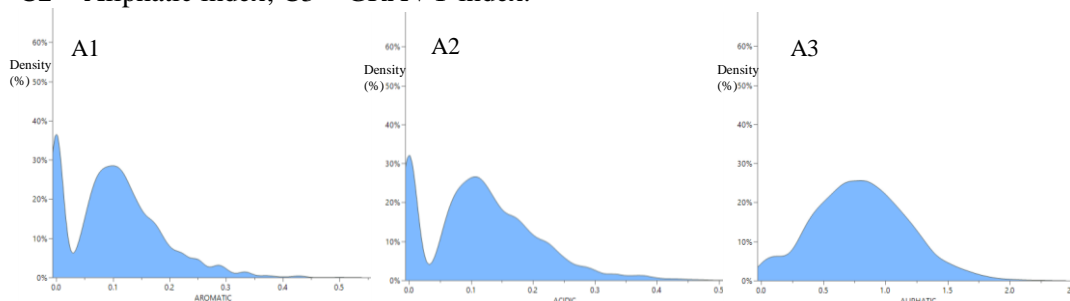
657  
 658 **Figure 2:** Categorization of the 3,005 unique peptides identified via UHPLC-MS/MS based on protein  
 659 origin (threshold for peptide number: 24).  
 660



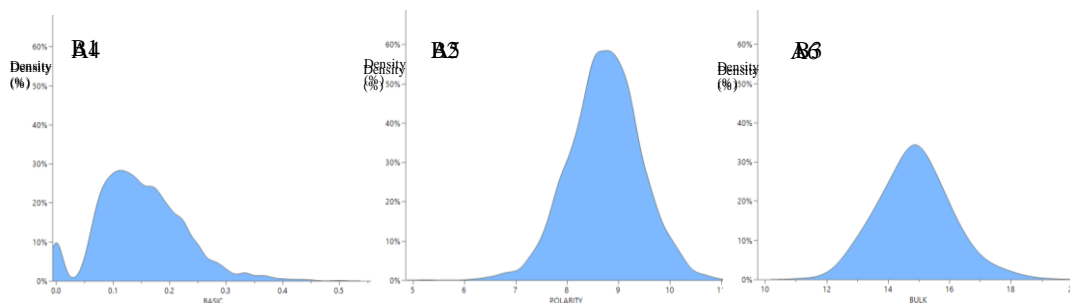
661

663 **Figure 3** : A) Distribution of the overall 3,561 peptides on the 28 solutions (normalized distribution, kernel  
 664 density): A1 = Relative aromatic nature; A2 = Relative acidic nature; A3 = Aliphatic index; A4 = Relative  
 665 basic nature; A5 = Polarity; A6 = Bulk; A7 = GRAVY index; A8 = Length; A9 = Charge.  
 666 B) Comparison of distributions of the overall 3,561 peptides (normalized distribution, kernel density): B1 =  
 667 Charge with 50Ib-50W in blue; 100Rb in green and 100Pb in red; B2 = Charge with 50Ia-50W in blue; 100Ra  
 668 in green and 100Pa in red; B3 = Polarity with Refa in yellow and Refb in orange.  
 669 C) Comparison of distributions of the overall peptides (3,561 peptides in blue) and for the peptides correlated  
 670 to bitterness (275 peptides in red) on the 28 solutions (normalized distribution, kernel density): C1 = Polarity;  
 671 C2 = Aliphatic index; C3 = GRAVY index.

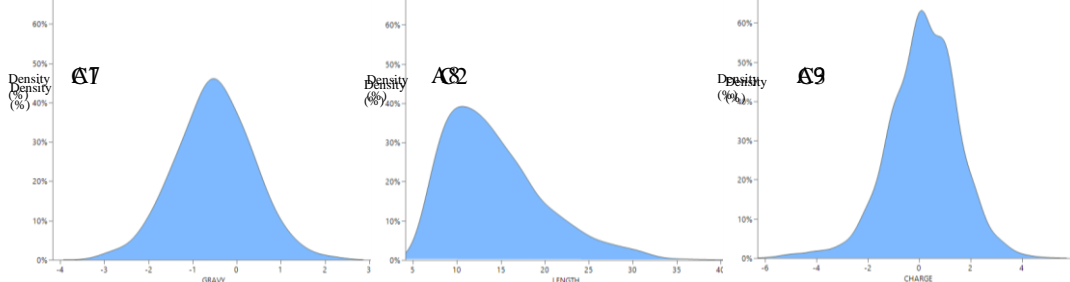
672



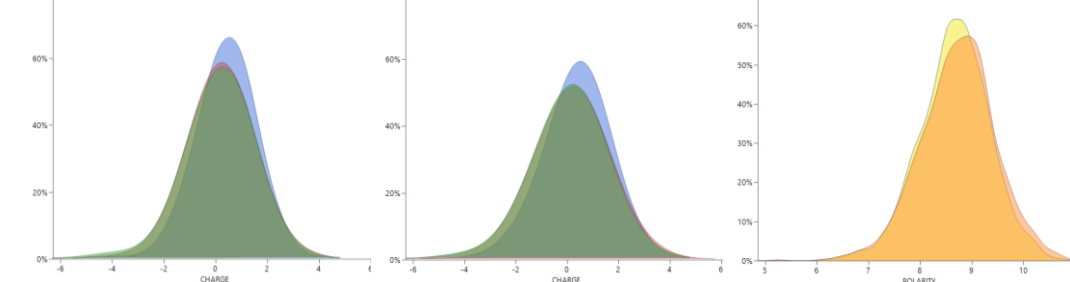
673



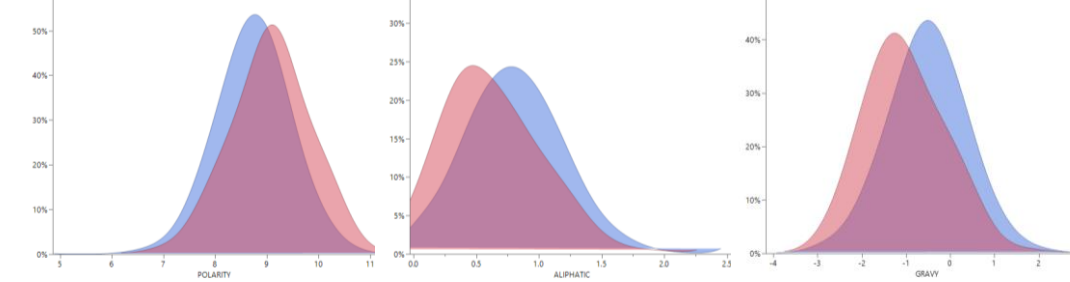
674



675

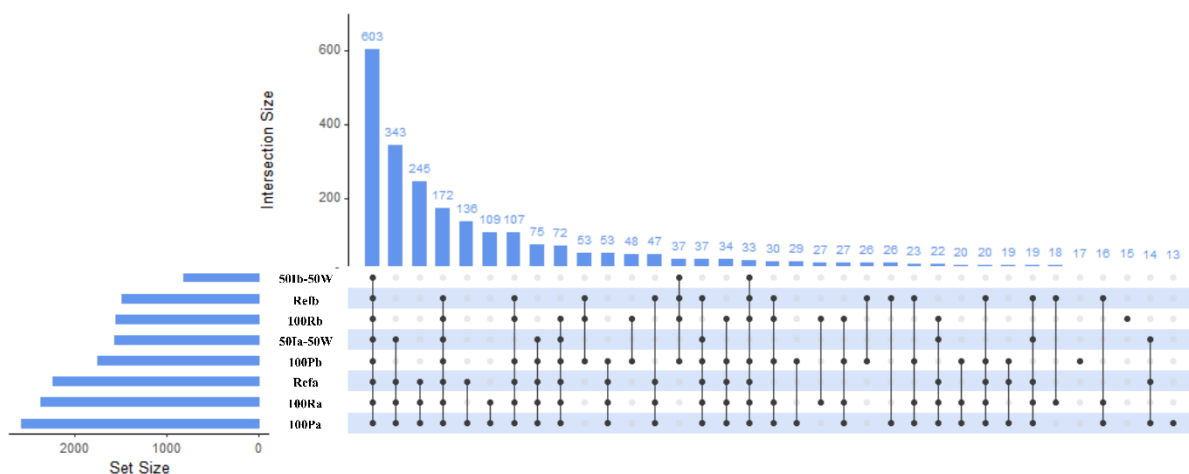


676



677 **Figure 4:** Depiction of the intersections in peptide sets among the six fractions and the two raw solutions  
 678 (UpSet plot). The blue horizontal bars show the number of peptides in each fraction/solution. The black dots  
 679 and lines show the combinations of peptides that make up each cluster or subset of the fractions/solutions. The  
 680 vertical histogram shows the number of peptides in each subset.

681  
 682



683  
 684

685  
 686

687  
 688

689  
 690

691  
 692

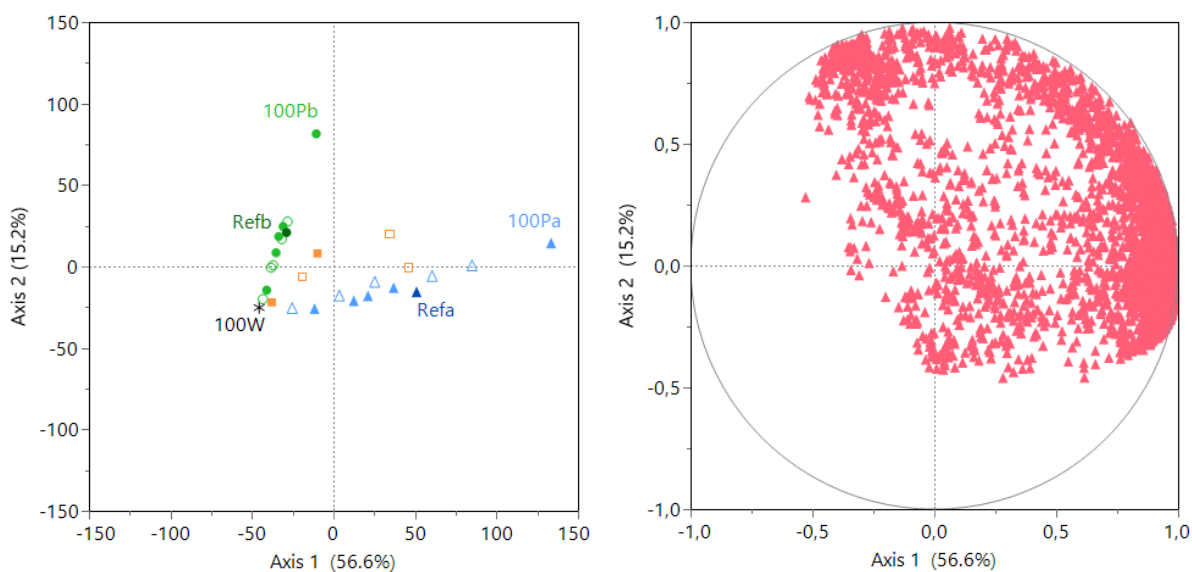
693  
 694

695  
 696

697  
 698

699  
 700

701 **Figure 5:** Results of the principal component analysis (PCA, wide method) examining the peptide profiles for  
702 the 28 solutions, which were determined using a fraction-based formulation strategy and the peptides that had  
703 been identified (based on 3,561 peptides). On the left is a loading plot showing the correlational relationships  
704 between the PCA axes 1 and 2 and the peptide areas. On the right is a PCA plot with the same two axes that  
705 shows the relative similarity in the solutions' peptide profiles. The green circles are the recombined solutions  
706 created from batch b. The blue triangles are the recombined solutions created from batch a. The orange  
707 squares are the recombined solutions created from batch a and batch b. The dark star is the water solution. The  
708 solid symbols represent the measured values, and the empty symbols represent the calculated values.  
709



710

711

712

713 **Captions to Supplementary Tables**

714

715 **Supplementary Table 1:** Composition of the 28 solutions used in this study, which were created by mixing  
716 permeates a and b, retentates a and b, and pellets a and b. For the coding: Refa (respectively Refb) correspond  
717 to the solutions of pea protein isolates a (resp. b) at 4% (w/w); “Pa” (resp. “Pb”) mean permeate from Refa  
718 (resp. from Refb), “Ia” (resp. “Ib”) mean Pellet from Refa (resp. from Refb), “Ra” (resp. “Rb”) mean  
719 Retentate from Refa (resp. from Refb) and “W” mean water. For example, “X Pb-Y Ra” mean “Recombined  
720 product constituted of X% of permeate from Refb and Y% of retentate from Refa”.

721

722 **Supplementary Table 2:** Peptides identified in the pea protein solutions that had sequences homologous to  
723 those of previously described antioxidant peptides (BIOPEP database) (Iwaniak et al., 2016).

724

725

726 **Supplementary Table 1:**

<b>Solution ID</b>	<b>Permeate a (%)</b>	<b>Permeate b (%)</b>	<b>Retentate a (%)</b>	<b>Retentate b (%)</b>	<b>Pellet a (%)</b>	<b>Pellet b (%)</b>	<b>Water (%)</b>
100W	0	0	0	0	0	0	100
25Ib-75W	0	0	0	0	0	25	75
50Ib-50W	0	0	0	0	0	50	50
30Ia-70W	0	0	0	0	30	0	70
50Ia-50W	0	0	0	0	50	0	50
40Rb-30Ib-30W	0	0	0	40	0	30	30
40Rb-30Ia-30W	0	0	0	40	30	0	30
50Rb-50W	0	0	0	50	0	0	50
100Rb	0	0	0	100	0	0	0
40Ra-30Ib-30W	0	0	40	0	0	30	30
50Ra-25Ia-25W	0	0	50	0	25	0	25
60Ra-40W	0	0	60	0	0	0	40
100Ra	0	0	100	0	0	0	0
40Pb-60W	0	40	0	0	0	0	60
Refb	0	40	0	36	0	24	0
50Pb-50W	0	50	0	0	0	0	50
50Pb-25Ib-25W	0	50	0	0	0	25	25
50Pb-50Rb	0	50	0	50	0	0	0
70Pb-30Ra	0	70	30	0	0	0	0
100Pb	0	100	0	0	0	0	0
25Pa-25Ra-13Ia-38W	25	0	25	0	12.5	0	37.5
Refa	38	0	34	0	28	0	0
40Pa-60W	40	0	0	0	0	0	60
40Pa-60Rb	40	0	0	60	0	0	0
50Pa-25Ib-25W	50	0	0	0	0	25	25
50Pa-1a25-W25	50	0	0	0	25	0	25
50Pa-50Ra	50	0	50	0	0	0	0
100Pa	100	0	0	0	0	0	0

727

728 **Supplementary Table 2:**

Antioxidative sequence	Protein	Peptide identified in this study
ADGF	Lectin	SYNVADGFTFF
		VINAPNSYNVADGFT
		VINAPNSYNVADGFTF
		VINAPNSYNVADGFTFF
ADVFNPR	Legumin L1 beta chain	HEDLAGSSQADVFNPRAGRIT
		HEDLAGSSQADVFNPRAGRITSVN
		HEDLAGSSQADVFNPRAGRITSVNSLT
		HEDLAGSSQADVFNPRAGRITSVNSLTL
		HEDLAGSSQADVFNPRAGRITSVNSLTLPLVK
		HEDLAGSSQADVFNPRAGRITSVNSLTLPLVKL
		LKLHEDLAGSSQADVFNPRAGRITSVN
		LKLHEDLAGSSQADVFNPRAGRITSVNSLT
ELLI	Histone H3.2	STELLIR
FVPH	PsRT17-1	VFVPHIRTLGD
		VFVPHIRTLGDA
FVPH and SAEHGSLH	Legumin A2	SAEHGSLHKNAM(MOD:00719)FVPH
		SAEHGSLHKNAM(MOD:00719)FVPHY
HLHP	Sucrose transport protein	QLSGAFKELKRPM(MOD:00719)W
KFPE	PIP1-2	M(MOD:00719,MOD:00408)EAKEEDVSLGANKFPERQPIG
		M(MOD:00719,MOD:00408)EAKEQDVSLGANKFPERQPLG
KFPE	PIP-type 7a	M(MOD:00408)EAKEQDVSLGANKFPERQPLG
LPILR	Legumin (Minor small)	LPILRN
		LPILRNL
		SGAGRISTVNSLTLPILR
		SGAGRISTVNSLTLPILRN
		SGAGRISTVNSLTLPILRNL
SGAF	Malate dehydrogenase	Q(MOD:01160)RIARISAPHLHPSN
YLKT	Seed linoleate 9S-lipoxygenase-3	VKSPQKAYLKTITP
		VKSPQKAYLKTITPKFQT
		YLKTITP
YVGD	Actin-3	AYVGDEAQSQRGILT

729

730 **Captions to Supplementary Figures**

731 **Supplementary Figure 1:** General workflow of the different steps of the study analysis.

732 **Supplementary Figure 2:** Total Ion Chromatogram (TIC) from 100Pa sample.

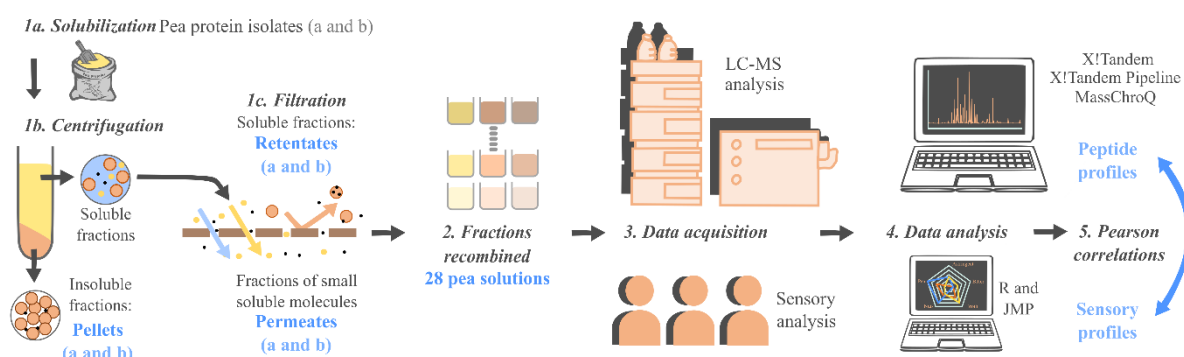
733 **Supplementary Figure 3:** Peptides (size < 8 residues) correlated with perceived bitterness (score out of 10);  
734 the R<sup>2</sup> values and p-values from the Pearson's correlational analysis are indicated.

735

736 **Supplementary Figure 1:** General workflow of the different steps of the study analysis

737

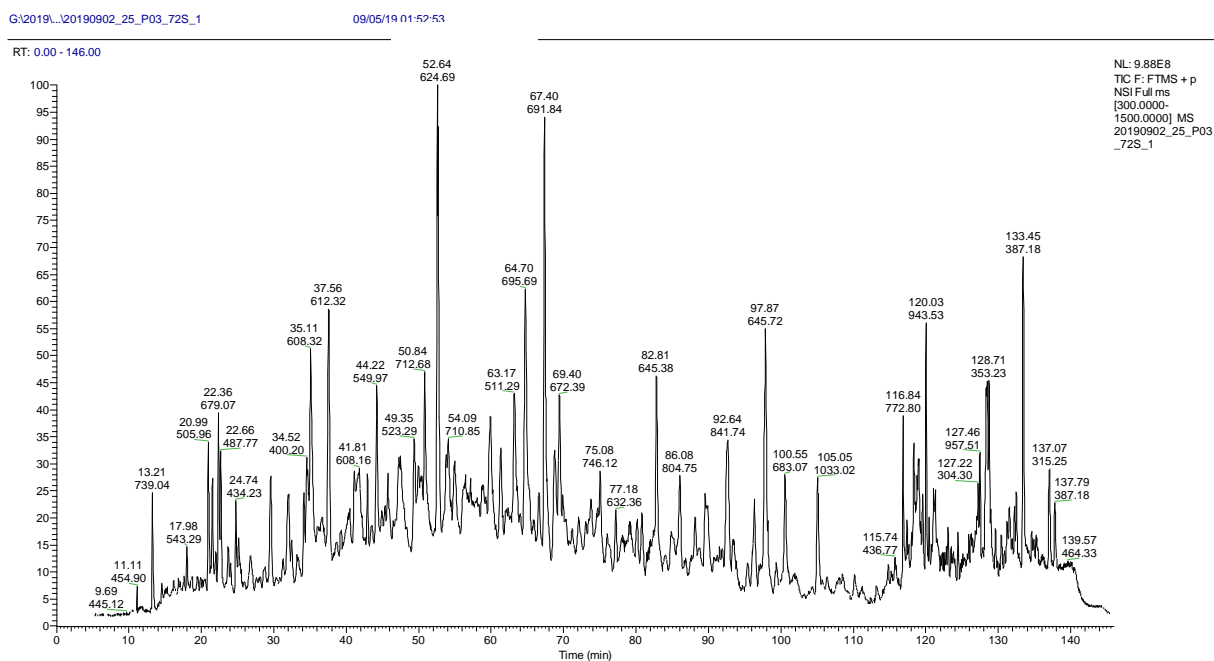
738



740

741

742 **Supplementary Figure 2:** Total Ion Chromatogram (TIC) from 100Pa sample



744 **Supplementary Figure 3: Peptides (size < 8 residues) correlated with perceived bitterness (score out of 10);**

745 the R<sup>2</sup> values and p-values from the Pearson's correlational analysis are indicated

746

747

748

749

750

751

752

753

754

